



Assessing avocado firmness at different dehydration levels in a multi-sensor framework

Puneet Mishra^{a,*}, Maxence Paillart^a, Lydia Meesters^a, Ernst Woltering^{a,b}, Aneesh Chauhan^a, Gerrit Polder^c

^a Wageningen Food and Biobased Research, Bornse Weiland 9, P.O. Box 17, Wageningen 6700AA, the Netherlands

^b Horticulture and Product Physiology Group, Wageningen University, Droevendaalsesteeg 1, P.O. Box 630, Wageningen 6700AP, the Netherlands

^c Greenhouse Horticulture Group, Wageningen University & Research, P.O. Box 644, Wageningen 6700AP, the Netherlands

ARTICLE INFO

Keywords:

Sensor-fusion
Chemometrics
Variable selection
Fruit quality

ABSTRACT

This study aims to utilize non-destructive sensing based on Vis-NIR spectroscopy and acoustic to predict firmness of avocado fruit. The study has three aims, the first aim was to find the best reference firmness measurement technique for calibrating Vis-NIR spectroscopy data related to avocado ripening i.e., acoustic firmness (AF), limited compression (LC) and penetrometer max force (Fmax). The second aim was to study the generalizability of Vis-NIR models with respect to the dehydration level of avocado fruits. Dehydration of outer skin during storage is common and may cause model failure as the Vis-NIR signal is dominated by signal corresponding to high moisture in fresh fruit. The third aim was to fuse the Vis-NIR spectroscopy and acoustic information to improve the prediction of the LC and Fmax, otherwise unattainable with a single technique. The results showed that the best models for firmness prediction were obtained with LC as the reference. The avocado skin dehydration negatively affected the performance of Vis-NIR models to predict firmness. Further, a fusion of Vis-NIR spectroscopy and acoustic information improved prediction (reduced error by 21%) of firmness in avocado. Assessing avocado firmness in a multi-sensor framework can allow to precisely access the ripeness stage of avocados.

1. Introduction

Rapid non-destructive estimation of fruit quality allows the best management of fruit supply chain, starting from harvest up to the consumer [1][2]. Fruit quality parameters such as dry matter (DM), soluble solids content (SSC) and firmness are of key importance and supply indirect access to fruit maturity and quality levels [3]. Several non-destructive techniques such as acoustic analysis[4], near-infrared spectroscopy (NIRS) [3], hyperspectral imaging (HSI) [5–7], X-ray imaging [8,9], magnetic resonance imaging [10,11], Raman spectroscopy [12] and optical coherence tomography [13] are widely explored for estimating the fruit quality.

Avocado being a highly commercially attractive fruit has always been of interest for the application of non-destructive technologies. There are two main stages at which the non-destructive sensing can be deployed in the case of avocado i.e., to decide on the best harvest time and to access its maturity during ripening under storage. DM is the key quality trait that is predicted using the near-infrared (NIR) sensors for

making the best harvest decisions [14]. DM shows a good correlation with the oil content, which is the most important avocado quality trait [15]. Avocados are harvested hard green and soften during the storage and later shelf life. The softening rate is moderate at the beginning, increases later and stops at maturity [16]. Studies have shown that a proper prediction of avocado firmness allows estimation of its maturity and expected storage time [15]. However, avocado has always been a challenging fruit to access its properties non-destructively in the post-harvest stage. A reason for that is unlike other fruit such as grape, apple and pear, the outer skin of the avocado is thick, thus, limiting the non-invasive techniques to properly access the fruit status beneath the skin. Further, of all the properties, the non-destructive firmness measurement has been a key challenging task as the non-contact techniques, such as near-infrared (NIR) spectroscopy, must rely on the secondary correlations between the signal and the firmness [3]. Although no single non-destructive sensing technology can be found as a perfect solution for the assessment of avocado firmness, sensing techniques have the potential to explain the firmness up to a certain extent. Some techniques

* Corresponding author.

E-mail address: puneet.mishra@wur.nl (P. Mishra).

<https://doi.org/10.1016/j.infrared.2021.103901>

Received 5 March 2021; Received in revised form 6 July 2021; Accepted 6 September 2021

Available online 8 September 2021

1350-4495/© 2021 The Author(s). Published by Elsevier B.V. This is an open access article under the CC BY license (<http://creativecommons.org/licenses/by/4.0/>).

can be found in relation to non-destructive firmness prediction of avocado fruit such as acoustics [17,18], low mass impact sensor [19], portable NIR spectroscopy [20] and laser doppler vibrometer (LDV) [21]. All these techniques supply an estimation of avocado firmness but are still too limited in their performance to be integrated with real-life commercial sorting line scenario or for routine analysis of avocado firmness in a non-destructive way.

In recent years, a large focus is gaining related to the integration of multiple sensors and data fusion for improved prediction of fruit and food quality [22–26]. It shows that using multiple sensors helps to improve the accuracy of prediction of fruit quality parameters compared to the use of a single sensor [27,26]. For example, improved prediction of apple firmness (~19 % reduction in error) and total soluble solids (TSS) content (~6 % reduction in error) was obtained by fusing the information from 4 different non-destructive sensors i.e., acoustic firmness, bio-yield firmness, visible and shortwave-infrared, and spectral scattering [28]. Improved prediction of colony-forming units in the strawberry fruit was obtained by combining the hyperspectral imaging and the electric nose signals [29].

A major limitation of correlation-based non-destructive sensing (single sensor or multi-sensor) is that they need reference measurements beforehand [3]. The reference measurements are used to calibrate the non-destructive techniques with data modelling approaches [30]. In the case of fruit, when it comes to reference measurement for firmness, the standard reference techniques are not well defined. Several options such as acoustic firmness (AF), penetrometer based max force measurement and limited compression are available [31]. It is, therefore, a challenge, to decide on a single technique which can be used as a standard reference measurement to calibrate non-destructive sensors.

This study has three main aims, the first aim was to find the best reference firmness measurement technique for calibration of Vis-NIR spectroscopy data during avocado ripening. Three commonly used approaches i.e., acoustic firmness (AF), limited compression (LC) and penetrometer max force (Fmax), were compared. The second aim was to study the generalizability of Vis-NIR models with respect to the dehydration level of avocado fruits. Dehydration of outer skin in fresh fruit during storage is common and may lead to model failure of Vis-NIR models as the Vis-NIR signal is dominated by signal corresponding to high moisture in fresh fruit. The third aim was to fuse the Vis-NIR spectroscopy and acoustic firmness data to improve on the prediction of the firmness, otherwise unattainable with a single technique. A fusion of acoustic and Vis-NIR is explored as both the techniques are minimally invasive and have a huge interest from commercial sorting line manufacturing industries. The chemometric modelling was performed using the partial least-squares (PLS) regression and the models were optimized using the wavelengths selection. A fusion of Vis-NIR spectroscopy and acoustic firmness data was performed in a mid-level data fusion perspective, where the key features extracted from the Vis-NIR data were combined with the acoustic signal and a multi-linear regression was performed. In this study, the acoustic and NIR combined model were explored for two main reasons, the first was that both techniques are non-destructive and provide complementary information [32]. The second reason was that many fresh fruit sorting machine developers integrate acoustics and NIR sensing technologies in their machines, hence, presenting the application of acoustic + NIR for avocado is also of commercial interest.

2. Material and methods

2.1. Avocado samples and storage treatment

Avocados (480 fruit) from South Africa (cultivar HASS, size 22, harvested in April 2020) were bought directly at a Dutch importer and transported to the post-harvest research facilities at Wageningen University & Research, The Netherlands. Fruit were kept at 5 °C and 85% relative humidity (RH). Fruit were randomly distributed to 6 batches of

80 fruit each (total 480 fruit). Each avocado received a unique code to compare several reference measurements with the corresponding Vis-NIR spectra. Furthermore, two measurement areas were delimited at the equator of each fruit with 90° side difference between the two areas. The first side (A) was used for acoustic measurements, limited compression, and DM content, the second side (B) for acoustic firmness and penetrometer max force measurement. Avocado should ideally be ripened under high relative humidity to prevent excessive water loss and structural changes in the peel [33,34]. Three batches were stored under dry conditions (20 °C and 45% RH) to trigger skin dehydration symptoms and the other three under best ripening conditions (20 °C and 90% RH). Overall, the experiment duration was 6 days and avocados were analyzed on 2nd, 4th, and 6th days. In the following sections, the fruit batches stored at 45 % RH and measured at 2nd, 4th and 6th days of storage will be denoted as Batch 1, Batch 2, and Batch 3. The fruit batches stored at 90 % RH and measured at 2nd, 4th and 6th days of storage will be denoted as Batch 4, Batch 5, and Batch 6.

2.2. Visible and near-infrared spectroscopy measurements

Spectral measurements were performed with a Hi-Res LabSpec spectrometer (ASD, USA). The data was acquired in the diffuse reflectance mode and in the spectral range of 350–2500 nm. The measurements were performed using the area scan probe (Hi-Brite probe) with a spot size of 10 mm on the same two positions where the reference measurements were done. The probe has an inbuilt 6.5 W halogen light source for illumination and the optical fibers to capture the reflected light. The instrument was controlled using the Indico Pro software, ASD, USA. The integration time was automatically optimized by the Indico Pro software and was defined as 15 ms. Each measurement was an average of ~ 5 consecutive measurements (at the same spot) automatically performed by the Indico Pro software. The white reference used was a Spectralon white standard. The radiometric calibration with white and dark reference was performed automatically by the Indico Pro software and the data were obtained as raw reflectance spectra. The radiometric calibration was performed as per Eq (1).

$$Reflectance = \frac{S - D}{W - D} \quad (1)$$

where S is fruit spectra, D is dark reference spectra and W is white reference spectra. The ASD (Analytical Spectral Devices) files were converted to MATLAB format with the help of The Unscrambler X 10.4, Camo Software's, USA (United States of America). The extracted data were saved in MATLAB format and were used for the data analysis. All the data analysis related to data fusion was performed in MATLAB 2018b (Natick, MA, USA). A summary of measurements process is

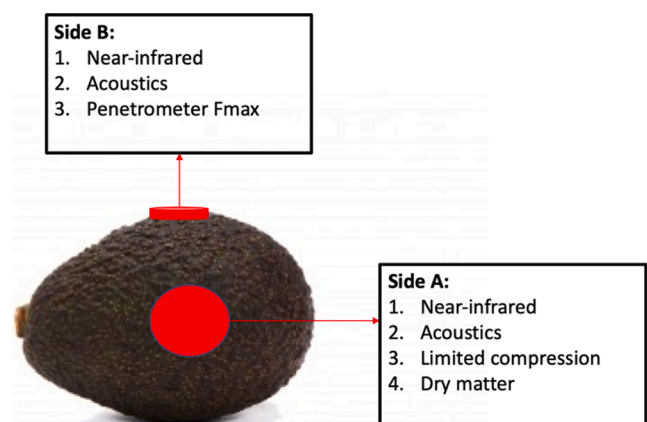


Fig. 1. A summary of measurements process on the avocado fruit during the experiment. The numbering in the figure represents the order of measurements.

shown in Fig. 1. A key point to note is that the reference measurements were not performed in replicate for the same fruit, hence, this work lacks information about the standard error of measurement for different reference analysis such as dry matter and firmness.

2.3. Reference measurements

2.3.1. Acoustic firmness sensing

The reference fruit firmness was measured with Aweta acoustic firmness sensor (AFS) (Aweta G & P B.V., The Netherlands). The AFS utilizes a gentle tap on the fruit and a microphone to record the acoustic signal generated by the tap. Further, it performs Fourier analysis to find the natural frequency (f) of the fruits and combines it with the fruit weight (w) to estimate the fruit firmness/toughness as $\text{firmness} = f^2 \times w^{2/3}$. For a single avocado, acoustic measurements were performed at two different spots (A and B) near the fruit belly at locations 90° apart. In addition, on the A spot, limited compression and DM were measured, and the B spot was used for the penetrometer (destructive) measurement of firmness.

2.3.2. Limited compression

Limited compression measurements were performed using a Fruit Texture analyzer (FTA) (Güss Manufacturing Ltd, Strand, South Africa) equipped with a 50 cm^2 flat probe and 25-kg load cell. Avocado with skin was set on a tripod, with equator side A directed to the probe. Maximal force was recorded at 3 mm final compression depth, with a crosshead speed of 5 mm s^{-1} . Maximal force was recorded by the FTAWin software (Güss Manufacturing Ltd, Strand, South Africa) and expressed in newtons (N).

2.3.3. Penetrometer

Penetrometer max force measurement was measured also with the Fruit Texture Analyzer instrument (Güss Manufacturing Ltd, Strand, South Africa). Depending on the fruit pulp texture, different partial hemispherical probes with area of 0.116, 0.5, 1 and 2 cm^2 were used; results were normalized and expressed in Newtons (N). On side B, avocado skin was first removed with sharp potato peeler, avocado with side B directed to the probe was set on a tripod, and maximal force was recorded at 8.9 mm final penetration depth, with a crosshead speed of 5 mm s^{-1} . Maximal force was recorded by the FTAWin software (Güss Manufacturing Ltd, Strand, South Africa).

2.3.4. Dry matter

Skin and pulp DM were investigated on the side A of avocado. Skin and pulp tissue samples were collected with a cork borer of 1.6 cm diameter. Staying stone tissue was discarded; skin and pulp tissue were carefully untied from each other with a sharp knife. Tissues were placed into clean aluminum cups and weights were recorded with a 3-digit analytical balance (Mettler-Toledo GmbH, Giessen, Germany) before and after drying in a hot-air oven (FD 56, Binder GmbH, Tuttlingen, Germany) at 80°C for 60 h. DM of each tissue was expressed in percentage (%).

2.3.5 wt. loss

Weight of individual avocado was recorded by the AFS. Weight loss was calculated by comparing the weight recording on evaluation day with first weight measured on day 0. Weight loss was expressed in percentage (%).

2.4. 2-way analysis of variance analysis

The study involved two main factors i.e., two humidity levels and three separate days of measurements. Hence, to understand the effect of two factors and their interaction on several measured traits, a 2-way analysis of variance (2-way ANOVA) was implemented. The 2-way analysis of variance was implemented by using the 'anovan' function

in MATLAB (2018b, Natick, MA, USA).

2.5. Spectral data analysis

All the measurements resulted in a total of 960 spectral measurements from 6 batches of 80 samples measured at 2 spots. The corresponding reference measurements were: 960 acoustic firmness measurements performed at exactly the same spot as spectral measurements, 480 limited compression measurements performed at the side A of fruits, 480 penetrometer Fmax measurements performed at side B of the fruit and 480 DM measurements performed on samples extracted from spot A. A key point to note is that although the spectra were measured on two spots on each fruit, the reference properties were measured on at one spot (either side A or B). Hence, the models were made between 480 fruit spectra and the reference property measured at the same spot. Although the spectral measurements were performed at two spots on fruit surface, however, the NIR data modelling was performed with the single spot measurement. This was done as fruit are highly heterogeneous and there is often high variation in the physico-chemical properties at different location on fruit surface. Hence, to avoid such heterogeneity to affect in the NIR data modelling, the modelling was based on the NIR spectra and property measured at the exact same spot of the NIR measurements.

2.5.1. Spectral data pre-processing

The spectra were obtained as reflectance. The spectra were normalized for global differences in intensities by estimating the standard normal variate (SNV) [35]. Further, Savitzky-Golay 2nd derivative was used for unrevealing the underlying peaks on the SNV corrected data [36]. Since models were explored for different dehydration levels, the spectra corresponding to each dehydration level were partitioned into calibration (60 %) and test (40 %) set using the Kennard-Stone (KS) algorithm [37]. The calibration set was used for model development while the test set was used for independent test of the model. A summary of different firmness measurement after partition is presented in Table 1.

2.5.2. Partial least-squares regression

PLSR is a commonly used chemometric technique for calibration on Vis-NIR data [30]. PLSR deals with the multi-co-linearity in the multi-variate Vis-NIR data by extracting the underlying peaks as the latent variables (LVs) [38,39]. The LVs were extracted having maximum covariance with the response variables. PLSR extracts a set of scores which are based on the projection of the data into the direction of LVs. In the present work, PLSR was implemented with the MATLAB's 'plsregress' function from statistics and machine learning toolbox. Further, a 10-fold cross-validation approach was integrated for optimizing the LVs. The LVs were selected by identifying the inflection point of the cross-validation error plot.

2.5.3. BOSS variable selection

Bootstrapping soft shrinkage (BOSS) is a recently developed

Table 1

A summary of firmness measurements in the calibration and test set after Kennard-Stone splitting. The distinct types of firmness measurements were acoustic firmness (AF), limited compression (LC) and max force (Fmax). Dry matter (DM) was measured on both fruit flesh and skin.

Firmness	Calibration set		Test set	
	Dehydrated	Non-dehydrated	Dehydrated	Non-dehydrated
AF ($\text{Hz}^2 \cdot \text{g}^{2/3}$)	15.18 ± 7.74	16.60 ± 8.19	13.43 ± 5.96	17.66 ± 7.46
LC (N)	47.10 ± 24.40	48.40 ± 25.30	42.28 ± 20.37	52.44 ± 24.84
Fmax (N)	42.74 ± 46.91	33.44 ± 44.41	38.58 ± 45.51	36.95 ± 38.05

wavelength selection approach for highly colinear data such as Vis-NIR data [40]. In the domain of Vis-NIR spectroscopy, the BOSS method has already outperformed high performing variable selection methods such Monte Carlo uninformative variable elimination, competitive adaptive reweighted sampling, and genetic algorithm partial least squares. The BOSS method combines the ideas of weighted bootstrap sampling and model population analysis. The weights of variables are found based on the absolute values of regression coefficients. Weighted bootstrap sampling is applied according to the weights to generate sub-models and model population analysis is used to analyze the sub-models to update weights for variables. During optimization soft shrinkage is imposed, in which less important variables are assigned smaller weights. The algorithm runs iteratively and ends when the number of variables reaches one. The best RMSECV (root mean square error of CV) are kept and a new calibration was set up with the retained variables. The BOSS was implemented in MATLAB (2018b, Natick, MA, USA).

2.5.4. Data fusion

The data fusion of Vis-NIR and acoustic firmness was performed by stacking the Vis-NIR variables selected with the BOSS, and the acoustic firmness measurements. After stacking PLS regression was used for recalibration and testing. Prior to data fusion, the acoustic firmness measurements were auto scaled by subtracting the mean followed by division with the standard deviation.

3. Results

3.1. Reference measurements

A summary of reference measurements for samples treated under two different RH (45 and 90%) conditions is shown in Table 2 and a further ANOVA (analysis of variance) analysis for each measured trait is supplied as supplementary. Different RH treatments were given to fruit samples to cause dehydration of the samples for testing generalizability of Vis-NIR models. Further, the fruits were stored and analysed at 3 different days to induce the ripeness (covering a period of 6 days). The DM of fruit flesh was not affected by the storage at different RH levels (p value = 0.221 see supp. Table 4) as well as the ripening (p value = 0.519 see supp. Table 4) and the DM was kept at an average ~ 20% for

Table 2

A summary of properties measured on avocado fruit stored at two different relative humidity levels and during three measurement days. Batch 1, 2 and 3 corresponding to the fruit batches stored at 45 % RH and measured during the 2nd, 4th, and 6th day, respectively. Batch 4, 5 and 6 corresponding to the fruit batches stored at 90 % RH and measured during the 2nd, 4th and 6th day, respectively. The A and B indicated the two sides of avocados used for sampling. The distinct types of firmness measurements were acoustic firmness (AF), limited compression (LC) and max force (Fmax). Dry matter (DM) was measured on both fruit flesh and skin.

Properties	45 % relative humidity			90 % relative humidity		
	Batch 1 (mean ± std)	Batch 2 (mean ± std)	Batch 3 (mean ± std)	Batch 4 (mean ± std)	Batch 5 (mean ± std)	Batch 6 (mean ± std)
DM flesh (%)	20.47	21.49	21.10	21.25	20.61	20.34
(A)	± 2.22	± 2.64	± 3.20	± 2.56	± 2.64	± 2.52
DM skin (%)	28.57	29.78	32.43	29.28	29.15	29.23
(A)	± 2.26	± 2.46	± 4.55	± 2.72	± 2.52	± 2.10
Weight loss (%)	2.78 ± 0.66	N.R.	8.32 ± 1.29	2.23 ± 0.51	N.R.	4.28 ± 0.71
N.R. : Not recorded	72.35 ±	32.35 ±	30.26 ±	77.97 ±	38.14 ±	32.85 ±
LC (N) (A)	13.44	13.65	14.29	16.76	15.12	13.07
Fmax (N)	70.30	21.37	28.63	72.17	21.64	11.05
(B) AF	±	±	±	±	±	±
(Hz ² .g ^{2/3})	40.45	31.78	43.28	44.42	36.89	23.20
(A and B)	21.65 ± 4.86	12.04 ± 4.85	11.72 ± 6.04	25.09 ± 5.72	15.01 ± 5.87	12.15 ± 4.66

both the RH levels. The DM of skin was significantly affected (p value = 9.01×10^{-5} see supp. Table 5) by the storage at different RH levels as well as by the ripening during storage (p value = 1.83×10^{-8} see supp. Table 5). During storage at 45 % RH, the DM of the skin increased from ~ 28 % (2nd day) to ~ 32 % (6th day). The DM of the skin stayed similar at ~ 29% for the fruit stored at 90% RH. During the storage, all types of firmness measurements showed a significant decrease (Except the 6th day penetrometer measurements where the fruits were too soft and difficult to measure with the penetrometer) from the 2nd day to the 6th reflecting the fruit softening/ripening (p value = 0 see supp. Table 1, 2 and 3). However, the difference in RH has a less significant effect on the firmness compared to the ripening. Weight loss seen for the samples stored in 45 % RH was double compared to the samples stored in 90% RH showing that keeping the samples at low RH (45 %) induced the dehydration in fruit samples and particularly the dehydration of the fruit skin. Both humidity and ripening affected induced a significant weight loss (p value ~ 0 see supp. Table 6).

3.2. Correlations between dry matter's and firmness's

The correlation coefficients (please note that these are correlations (r) and not coefficients of determination (R^2) as presented during model evaluation stage) between DM measurements and the distinct types of firmness measurements for samples stored at 45 % RH and 90 % RH are shown in Table 3 and 4, respectively (all measurements on the 3 storage days combined). For both RH levels (45% and 90%), the DM of fruit flesh shows almost no correlation with DM of skin. Further, for both RH levels, both the DM of skin and flesh show no, or a low negative correlation with the distinct types of firmness measurements. For both the RH levels, the AF and LC has the highest correlation, followed by the LC and Fmax. AF and Fmax have a low correlation with respect to the correlation between AF and LC. The correlation between different type of firmness measurements was higher in general for the non-dehydrated samples (stored at 90 % RH) compared to the dehydrated samples (stored at 45 % RH). Point to be noted that the correlation between AF and Fmax is poor compared to the correlation between LC and Fmax, irrespective of LC and AF have a high correlation. A reason for this could be the distinct locations used for measuring the LC, AF and Fmax, where LC was measured on the side A and Fmax was measured on side B with respect to the AF.

3.3. Spectral profiles of avocado fruits

The mean spectral profiles (350–2500 nm) for the avocado fruits during the three experiment days are shown in Fig. 2. The complete profile is presented in Fig. 2A; the important sub-regions are divided into separate parts and are shown in Fig. 2B-E. Batch 1 includes the hard green avocados and the Batch 3 includes matured ripe avocados. In the visible range (Fig. 2B), the spectra showed the discolouration (Solid blue line to yellow dotted line) of the outer skin colour [41], which decreased from green to brown/black along with the fruit ripening i.e., from Batch 1 to Batch 3. In the NIR spectral range (Fig. 2C), a global increase in reflectance was seen as the fruit ripens i.e., Batch 1 (solid blue lines) to Batch 3 (dotted yellow lines). Further, three main peaks were found in the NIR spectral range (Fig. 2C). The spectral peaks in the range of 700–1000 nm are from a complex mixture of peaks related to 2nd overtones of OH, 3rd overtones of RNH₂, 3rd overtones of CH, CH₂, CH₃, and 3rd overtones of ArOH. The later may be related to OH attached to an aromatic ring [41]. The spectral peak in the range of 1000–1150 nm can be related to the 2nd overtones of RNH₂ and 2nd overtones of CH group attached to the aromatic ring [41]. The spectral peak between 1200 and 1300 nm can be related to 2nd overtones of CH bond [41]. In the short-wave infrared-1 (SWIR-1) spectral range (Fig. 2D), a global increase in reflectance is as the fruit ripens i.e., Batch 1 (solid blue lines) to Batch 3 (dotted yellow lines). Further, two main peaks were found in the SWIR-1 spectral range (Fig. 2D). The peak around 1680 nm can be

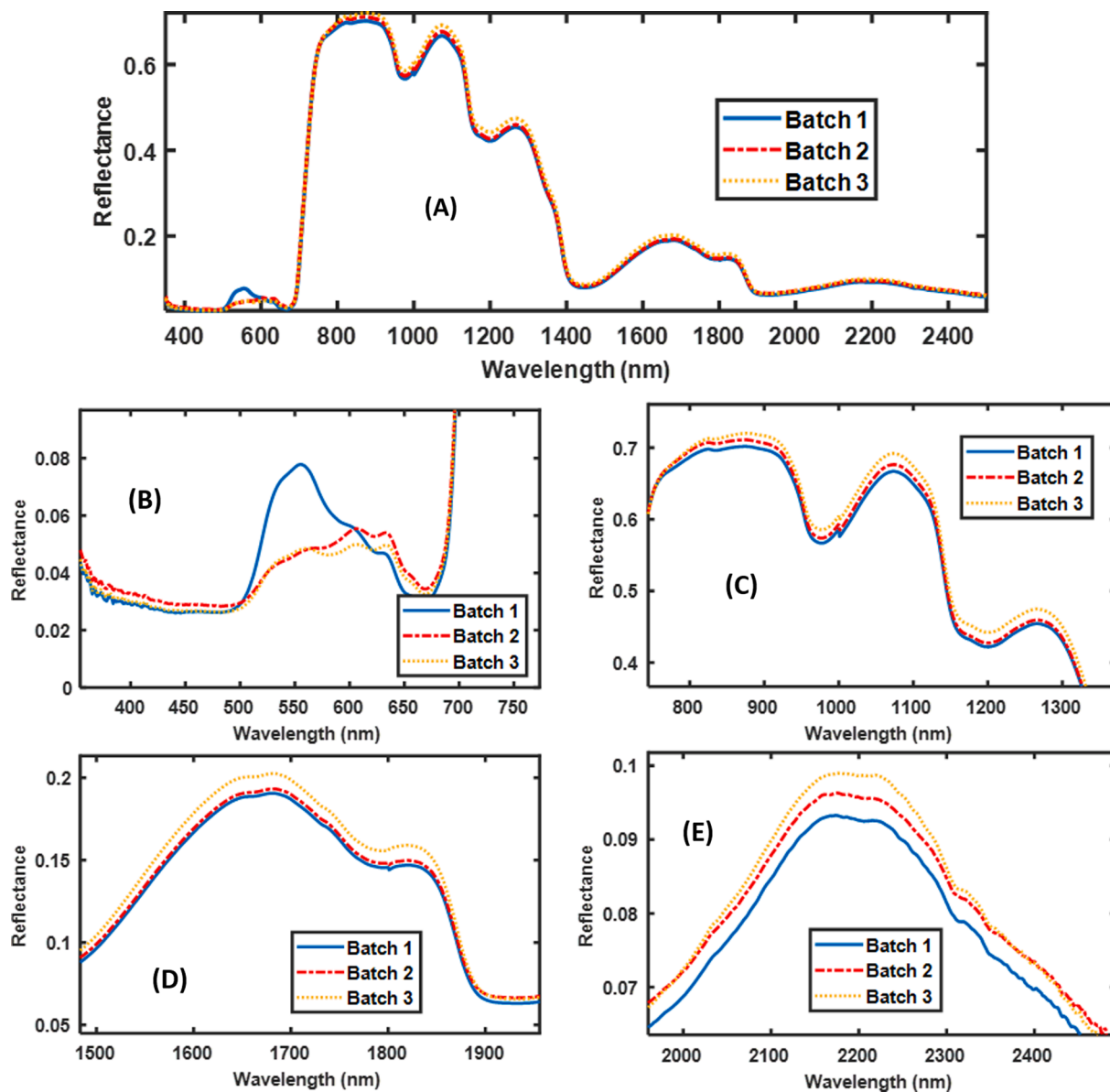


Fig. 2. The mean (80 fruit) spectral profiles of the avocado fruit during three experimental days (Batch 1 to 3). Spectra range: (A) 350–2500 nm, (B) 350–700 nm, (C) 750–1350 nm, (D) 1480–1950 nm, and (E) 1950–2450 nm.

related to the 1st overtones of CH_3 bond [41]. The peak around 1850 nm can be related to 1st overtones of RCO_2H [41]. In the short-wave infrared-2 (SWIR-2) spectral range (Fig. 2E), a global increase in reflectance was observed as the fruit ripens i.e., Batch 1 (solid blue lines) to Batch 3 (dotted yellow lines). Further, a single main peak (~ 2200 nm) in the SWIR-2 spectral range (Fig. 2E) corresponding to combination band vibration of CH_3 , CHO , RNH_2 and $\text{C} = \text{C}$ [41].

3.4. NIRS calibration for firmness (Global models with random samples from all batches)

The results of PLSR (Partial Least-Square Regression) global calibrations i.e., using samples from both 45 % and 90 %, tested individually for the respective data sets are shown in Fig. 3. Vis-NIR calibration using LC as the reference measurement had the highest R^2 for both dehydrated and non-dehydrated samples, compared to the AF and Fmax. Vis-NIR calibration using penetrometer Fmax as the reference has the second highest R^2 for both dehydrated and non-dehydrated samples. Vis-NIR calibration using AF as the reference had the lowest R^2 for both

dehydrated and non-dehydrated samples. A key point to note in Fig. 3E-F, is that the behaviour of the AF appear non-linear. This is because the AF measurements are less sensitive in explaining the firmness of too hard or too soft fruits. Similar, the Fmax measurement in this study also struggled for too soft fruit as most of the recording can be found accumulated in the range of 0–10 N (Fig. 3C-D).

3.5. Variable selection

The variable selection with BOSS improved the model predictive performance compared to the standard PLSR modelling (Fig. 4). The improvements were noted for both dehydrated and non-dehydrated samples. The improvements in the case of non-dehydrated samples were related to the decrease in RMSEP. The improvements in the case of dehydrated samples were related to the increase in R^2 and decrease in RMSEP. In the case of LC, the R^2 was increased from 0.73 to 0.78 and 0.86 to 0.87 for dehydrated and non-dehydrated samples, respectively. Further, the RMSEP was decreased from 10.5 to 9.5 N and 9.1 to 8.9 N for dehydrated and non-dehydrated samples, respectively. In the case of

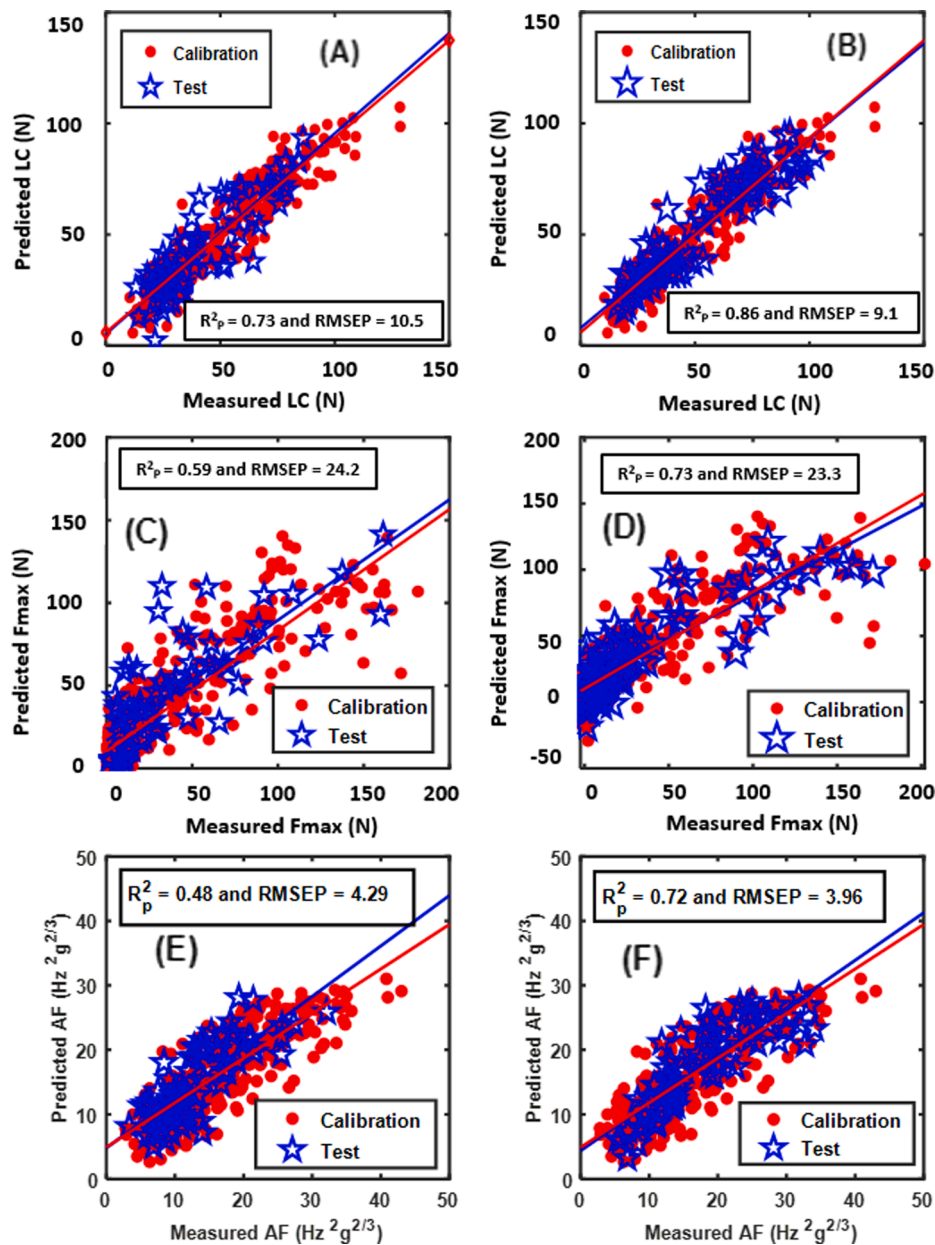


Fig. 3. Partial least-squares regression (PLSR) for 3 different reference firmness measurements with visible and near-infrared spectroscopy. The left and the right column are the 45 % and 90 % relative humidity (RH) samples. PLSR results for 45 % RH, (A) limited compression (LC) in Newtons (N), (C) penetrometer max force (Fmax) in Newtons (N), and (E) acoustic firmness (AF) in $\text{Hz}^2 \text{g}^{2/3}$. PLSR results for 90 % RH, (B) LC (N), (D) Fmax (N), and (F) AF ($\text{Hz}^2 \text{g}^{2/3}$).

Fmax, the R^2 was increased from 0.59 to 0.65 and 0.73 to 0.74 for dehydrated and non-dehydrated samples, respectively. Further, the RMSEP was decreased from 24.2 to 22.3 N and 23.3 to 22.9 N for dehydrated and non-dehydrated samples, respectively. In the case of AF, the R^2 was increased from 0.48 to 0.49 and 0.72 to 0.73 for dehydrated and non-dehydrated samples, respectively. Further, the RMSEP was decreased from 4.29 to 4.24 $\text{Hz}^2 \text{g}^{2/3}$ and 3.92 to 3.82 $\text{Hz}^2 \text{g}^{2/3}$ for dehydrated and non-dehydrated samples, respectively.

A summary of Vis-NIR wavelengths found by the BOSS variable selection approach for predicting values obtained by distinct types of firmness measurements is detailed in supplementary Table 7.

3.6. Mid-level data fusion of acoustic and near-infrared (Global models)

The mid-level data fusion of the BOSS selected Vis-NIR wavelengths and the AF measurements improved the predictive performance of Vis-

NIR models (Fig. 5). The improvements were noted for both the LC and Fmax. In the case of LC, the R^2 was increased from 0.78 to 0.82 and 0.87 to 0.89 for dehydrated and non-dehydrated samples, respectively. Further, the RMSEP was decreased from 9.5 to 9.0 N and 8.9 to 7.7 N for dehydrated and non-dehydrated samples, respectively. In the case of Fmax, the improvement was limited only to a decrease in RMSEP. The RMSEP's were decreased from 22.3 to 20.7 N and 22.9 to 20.0 N for dehydrated and non-dehydrated samples, respectively. A key point to note that in this study the RMSEP for the Fmax predictions were relatively higher compared to the LC predictions, hence, the models to predict Fmax in this study may not be practically relevant. Such poor performance of the Fmax was due to the skewed distribution of the fruit firmness where a lot more soft fruit were present compared to hard fruit.

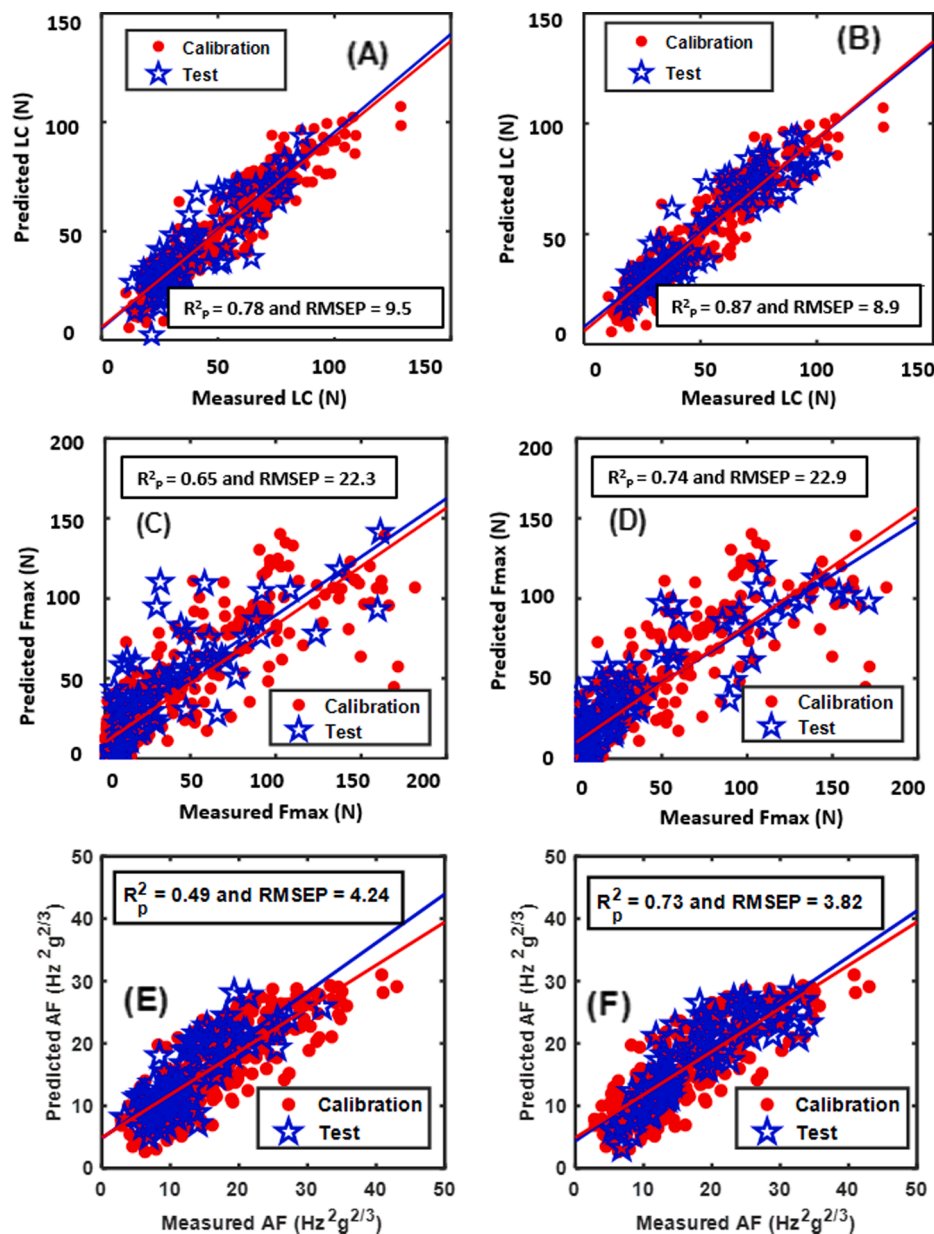


Fig. 4. Bootstrapping soft shrinkage (BOSS) modelling for 3 different reference firmness measurements with visible and near-infrared spectroscopy. The left and the right column are the 45 % and 90 % relative humidity samples. BOSS results for 45 % RH, (A) limited compression (LC) in Newtons (N), (C) penetrometer max force (Fmax) in Newtons (N), and (E) acoustic firmness (AF) in $\text{Hz}^2\text{g}^{2/3}$. BOSS results for 90 % RH, (B) LC (N), (D) Fmax (N), and (F) AF ($\text{Hz}^2\text{g}^{2/3}$).

4. Discussion

4.1. Key wavelengths and their relation with firmness

Vis-NIR spectroscopy for firmness prediction is challenging due to the absence of any direct correlation between functional group vibrations and the firmness, and in most of the cases, it is the secondary correlation that supports Vis-NIR spectroscopy to predict firmness. The study shows that the wavelengths for predicting firmness were not localized to functional group vibration overtones but were distributed over the full range of Vis-NIR spectroscopy (350–2500 nm), ranging from the visible part related to the chlorophyll degradation to SWIR part capturing the functional group vibration combinations and overtones of chemical bonds. Furthermore, variable selection for different firmness's showed that the selected wavelengths had a small subset of wavelengths in common. Such different selected wavelengths indicates that different firmness's may measure different structural properties of the tissue,

otherwise similar wavelengths would have been selected. However, LC and AF reached a high number of common wavelengths showing that AF and LC measure comparable properties. This is also emphasized by the fact that LC and AF values show high correlation (Table 3 and 4) compared to e.g., Fmax and AF.

The main wavelengths related to firmness selected in this study in the visible region (618–690 nm) are related to the degradation of green colour in the outer peel of the avocados. Such a loss of green colour occurs due to the degradation of chlorophyll content in the peel [42]. In the NIR part, the main firmness-associated wavelengths selected (~744 nm, ~875 nm, ~970 nm) could be related to fatty acids, sugars and moisture showing that firmness may have a secondary correlation with the change in fatty acid composition, moisture, and sugars. From the fruit physiology perspective, the enzymatic activity that loosens/destroys the cell wall matrix and cell to cell connections is the main cause associated with the softening of fruit [43,44]. However, since Vis-NIR spectroscopy cannot directly explain the enzymatic activity in the

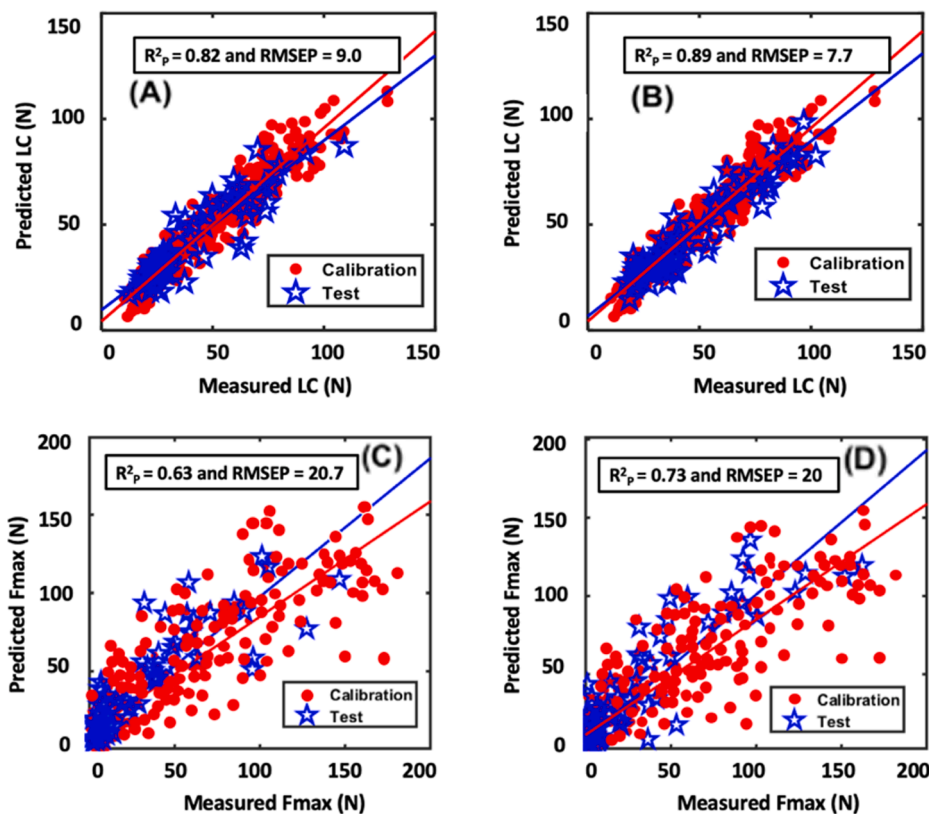


Fig. 5. Partial least-squares regression (PLSR) modelling on the fused visible and near-infrared (Vis-NIR) selected wavelengths and the acoustic firmness data to predict limited compression (LC) in Newtons (N) and penetrometer max force (Fmax) in Newtons (N). LC: (A) dehydrated samples (45 % RH) and (B) non-dehydrated samples (90 % RH). Fmax: (C) dehydrated samples (45 % RH) and (D) non-dehydrated samples (90 % RH).

fruit, it could be the secondary correlation to enzymatic activity that is captured by the Vis-NIR. To moisture, the loss of water (i.e., increase in DM) causes a decrease in cell turgor pressure, hence, decrease in the firmness of the fruit [45]. In this study, such a correlation was also noted where the DM showed a negative correlation with the firmness, however, the correlation was low (Table 3).

In relation to the fatty acids and sugars, the selected wavelengths agreed with the results reported related to the monitoring of avocado post-harvest ripening, where a significant difference in the fatty acid [46] and sugars composition were noted. During the ripening after harvest, the C₇ sugar disappears completely leaving the C₆ sugars [47]. In the SWIR1 part, the main wavelengths selected (~1200 nm, ~1420 nm, ~1700 nm, 1887 nm) can be related to the fatty acids, sugars, and proteins. In relation to protein, a recent study demonstrated that the total soluble protein content increases during the avocado fruit ripening [48]. In the SWIR2 part, the main wavelengths selected (~2300 nm) can be related to the combination wavelengths arising from fatty acids and sugar [49].

Table 3

A summary of correlation coefficients (r) between dry matter (DM) and several firmness measurements for samples stored at 45 % relative humidity (all measurements on the 3 days storage combined). The distinct types of firmness measurements were acoustic firmness (AF), limited compression (LC) and max force (Fmax).

Parameters	DM flesh (%)	DM skin (%)	AF (Hz ² g ^{2/3})	LC (N)	Fmax (N)
DM flesh (%)	1				
DM skin (%)	-0.01	1			
AF (Hz ² g ^{2/3})	-0.31	-0.15	1		
LC (N)	-0.31	-0.25	0.87	1	
Fmax (N)	-0.20	-0.11	0.58	0.73	1

Table 4

A summary of correlation coefficients (r) between dry matter (DM) and several firmness measurements for samples stored at 90 % relative humidity (all measurements on the 3 days storage combined). The distinct types of firmness measurements were acoustic firmness (AF), limited compression (LC) and max force (Fmax).

Parameters	DM flesh (%)	DM skin (%)	AF (Hz ² g ^{2/3})	LC (N)	Fmax (N)
DM flesh (%)	1				
DM skin (%)	-0.05	1			
AF (Hz ² g ^{2/3})	-0.18	0.12	1		
LC (N)	-0.14	0.08	0.89	1	
Fmax (N)	-0.09	0.04	0.65	0.80	1

4.2. Effect of dehydration on model performance

The storage of fruit at low RH (45 %) induced increased dehydration which was limited to the skin and not the fruit flesh. This is logical as the skin of the fruit was in direct contact with the environment and suffered most of the moisture loss. These results agree with [50], who reported only increase of skin DM and not of pulp DM during ripening of avocado under 61% RH. Skin dehydration affects the non-destructive sensing techniques such as AF which relies on generating a sound wave by affecting the fruit. A reason is that the elasticity of the fruit changes and this affects the signal captured by the AF techniques [51]. This is also clear in the current study as the correlation between the AF and Fmax was poorer for dehydrated samples compared to the non-dehydrated samples. Like AF, the LC (performed with fruit skin intact) also measures a mix of elastic and other texture properties related to the fruit skin and flesh [31]. In this study, the correlation between the LC and Fmax was poorer for dehydrated samples compared to the non-dehydrated

samples. However, the correlation of LC with penetrometer force max was much higher compared to the correlation between the AF and Fmax. This study showed that the DM of skin and flesh of the avocado fruit have low correlation with any kind of firmness's i.e., AF, LC and Fmax (Table 3 and 4), suggesting that DM is not a good indicator of fruit firmness [52].

4.3. Model performed the best for limited compression

In comparison to the three different firmness measurements used to calibrate the Vis-NIR spectral data, the LC reached the best model performance in terms of high R^2 and low RMSEP. Fmax is a widely used criterion to perform the reference firmness analysis of fresh fruit but this study shows it is not the best technique to perform the calibration of non-destructive sensors such as Vis-NIR spectroscopy. Further, AF measurements carry complementary information to the Vis-NIR spectroscopy and their fusion lead to improved prediction of both LC and Fmax. Similar improvements in firmness prediction of apples were also seen when the AF and Vis-NIR spectral data were fused [28,32]. The AF and LC share a major part of common information as they both are performed over the skin capturing the elastic properties of the skin. However, in this study, a combination of AF with the Vis-NIR improved the prediction of LC, showing the AF and Vis-NIR complementary information essential to reach a better non-destructive prediction of LC. Therefore, instead of using AF as a reference measurement, a better choice is to combine the AF measurement as a non-destructive tool for sensor fusion with Vis-NIR spectroscopy as also recommended in several earlier research [28,32].

5. Conclusions

Firmness prediction with Vis-NIR spectroscopy is a challenging task due to lack of any direct correlation with the functional group vibrations. Also, different reference firmness measurements correlate differently with the Vis-NIR spectroscopy data. This study supplied a sensor fusion based solution to obtain enhanced predictive models for avocado fruit firmness by fusing the Vis-NIR spectroscopy and acoustic firmness data. The specific conclusions from this study are:

1. Out of the three reference firmness techniques explored, the limited compression was found to be the best reference technique to calibrate with Vis-NIR spectroscopy sensor. A key point to note that in this study the Fmax distribution was skewed as after ripening treatment most of the fruit were in low firmness.
2. The dehydrated samples obtained higher RMSEP (Vis-NIR) compared to the non-dehydrated samples, showing that the dehydration of the samples effect the performance of Vis-NIR models for firmness prediction
3. The variable selection improved the model predictive performance compared to the standard PLSR modelling, suggesting that best variables selection should be explored for optimising Vis-NIR models.
4. The acoustic firmness reference should not be used as a reference technique but should be used as complementary tool with Vis-NIR spectroscopy to improve model predictive performance.
5. Multi-sensor fusion approach for firmness prediction can improve firmness prediction even when there is disturbance due skin dehydration

Declaration of Competing Interest

The authors declare that they have no known competing financial interests or personal relationships that could have appeared to influence the work reported in this paper.

Acknowledgments

The work acknowledges the 'ASD LabSpec' near-infrared spectrometer instrument used purchased under the project 'KB-38-001-008' financed by the Ministry of Agriculture, Nature and Food Quality, The Netherlands.

Appendix A. Supplementary material

Supplementary data to this article can be found online at <https://doi.org/10.1016/j.infrared.2021.103901>.

References

- [1] B.M. Nicolai, K. Beullens, E. Bobelyn, A. Peirs, W. Saeys, K.I. Theron, J. Lammertyn, Nondestructive measurement of fruit and vegetable quality by means of NIR spectroscopy: A review, *Postharvest Biol. Technol.* 46 (2) (2007) 99–118, <https://doi.org/10.1016/j.postharvbio.2007.06.024>.
- [2] K.B. Walsh, V.A. McGlone, D.H. Han, The uses of near infra-red spectroscopy in postharvest decision support: A review, *Postharvest Biol. Technol.* 163 (2020) 111139, <https://doi.org/10.1016/j.postharvbio.2020.111139>.
- [3] K.B. Walsh, J. Blasco, M. Zude-Sasse, X. Sun, Visible-NIR 'point' spectroscopy in postharvest fruit and vegetable assessment: The science behind three decades of commercial use, *Postharvest Biol. Technol.* 168 (2020) 111246, <https://doi.org/10.1016/j.postharvbio.2020.111246>.
- [4] A. Mizrach, Ultrasonic technology for quality evaluation of fresh fruit and vegetables in pre- and postharvest processes, *Postharvest Biol. Technol.* 48 (3) (2008) 315–330, <https://doi.org/10.1016/j.postharvbio.2007.10.018>.
- [5] B. Li, M. Cobo-Medina, J. Lecourt, N. Harrison, R.J. Harrison, J.V. Cross, Application of hyperspectral imaging for nondestructive measurement of plum quality attributes, *Postharvest Biol. Technol.* 141 (2018) 8–15, <https://doi.org/10.1016/j.postharvbio.2018.03.008>.
- [6] X.i. Tian, S. Fan, W. Huang, Z. Wang, J. Li, Detection of early decay on citrus using hyperspectral transmittance imaging technology coupled with principal component analysis and improved watershed segmentation algorithms, *Postharvest Biol. Technol.* 161 (2020) 111071, <https://doi.org/10.1016/j.postharvbio.2019.111071>.
- [7] H. Zhang, B. Zhan, F. Pan, W. Luo, Determination of soluble solids content in oranges using visible and near infrared full transmittance hyperspectral imaging with comparative analysis of models, *Postharvest Biol. Technol.* 163 (2020) 111148, <https://doi.org/10.1016/j.postharvbio.2020.111148>.
- [8] S. Janssen, P. Verboven, B. Nugraha, Z.i. Wang, M. Boone, I. Josipovic, B. M. Nicolai, 3D pore structure analysis of intact 'Braeburn' apples using X-ray micro-CT, *Postharvest Biol. Technol.* 159 (2020) 111014, <https://doi.org/10.1016/j.postharvbio.2019.111014>.
- [9] B. Nugraha, P. Verboven, S. Janssen, Z. Wang, B.M. Nicolai, Non-destructive porosity mapping of fruit and vegetables using X-ray CT, *Postharvest Biol. Technol.* 150 (2019) 80–88, <https://doi.org/10.1016/j.postharvbio.2018.12.016>.
- [10] C.J. Clark, P.D. Hockings, D.C. Joyce, R.A. Mazucco, Application of magnetic resonance imaging to pre- and post-harvest studies of fruits and vegetables, *Postharvest Biol. Technol.* 11 (1) (1997) 1–21, [https://doi.org/10.1016/S0925-5214\(97\)01413-0](https://doi.org/10.1016/S0925-5214(97)01413-0).
- [11] S. Qiao, Y. Tian, P. Song, K. He, S. Song, Analysis and detection of decayed blueberry by low field nuclear magnetic resonance and imaging, *Postharvest Biol. Technol.* 156 (2019) 110951, <https://doi.org/10.1016/j.postharvbio.2019.110951>.
- [12] J. Qin, M.S. Kim, K. Chao, S. Dhakal, B.-K. Cho, S. Lohumi, C. Mo, Y. Peng, M. Huang, Advances in Raman spectroscopy and imaging techniques for quality and safety inspection of horticultural products, *Postharvest Biol. Technol.* 149 (2019) 101–117, <https://doi.org/10.1016/j.postharvbio.2018.11.004>.
- [13] M. Li, S. Landahl, A.R. East, P. Verboven, L.A. Terry, Optical coherence tomography—A review of the opportunities and challenges for postharvest quality evaluation, *Postharvest Biol. Technol.* 150 (2019) 9–18, <https://doi.org/10.1016/j.postharvbio.2018.12.005>.
- [14] P.P. Subedi, K.B. Walsh, Assessment of avocado fruit dry matter content using portable near infrared spectroscopy: Method and instrumentation optimisation, *Postharvest Biol. Technol.* 161 (2020) 111078, <https://doi.org/10.1016/j.postharvbio.2019.111078>.
- [15] C.E. Lewis, The maturity of avocados—a general review, *J. Sci. Food Agric.* 29 (10) (1978) 857–866, <https://doi.org/10.1002/jsfa.2740291007>.
- [16] G. Zauberman, Y. Fuchs, Ripening processes in avocados stored in ethylene atmosphere in cold storage, *J. Amer. Soc. Hort. Sci* 98 (5) (1973) 477–480.
- [17] U. Flitsanov, A. Mizrach, A. Liberzon, M. Akerman, G. Zauberman, Measurement of avocado softening at various temperatures using ultrasound, *Postharvest Biol. Technol.* 20 (3) (2000) 279–286, [https://doi.org/10.1016/S0925-5214\(00\)00138-1](https://doi.org/10.1016/S0925-5214(00)00138-1).
- [18] A. Mizrach, U. Flitsanov, M. Akerman, G. Zauberman, Ultrasonic Measurements of Avocado Softening in Low-Temperature Storage, *IFAC Proceed. Vol.* 31 (9) (1998) 75–78, [https://doi.org/10.1016/S1474-6670\(17\)44032-8](https://doi.org/10.1016/S1474-6670(17)44032-8).
- [19] Howarth, M. S., Shmulevich, I., Raithatha, C., & Ioannides, Y. (2003). Online nondestructive avocado firmness assessment based on low-mass impact technique.

- [20] M. Li, Z.Q. Qian, B.W. Shi, J. Medicott, A. East, Evaluating the performance of a consumer scale SCiO (TM) molecular sensor to predict quality of horticultural products, *Postharvest Biol. Technol.* 145 (2018) 183–192, <https://doi.org/10.1016/j.postharvbio.2018.07.009>.
- [21] S. Landahl, L.A. Terry, Non-destructive discrimination of avocado fruit ripeness using laser Doppler vibrometry, *Biosyst. Eng.* 194 (2020) 251–260, <https://doi.org/10.1016/j.biosystemseng.2020.04.001>.
- [22] P. Mishra, A. Biancolillo, J.M. Roger, F. Marini, D.N. Rutledge, New data preprocessing trends based on ensemble of multiple preprocessing techniques, *TrAC Trends Anal. Chem.* 132 (2020) 116045, <https://doi.org/10.1016/j.trac.2020.116045>.
- [23] P. Mishra, F. Marini, B. Brouwer, J.M. Roger, A. Biancolillo, E. Woltering, E.-V. Echtelt, Sequential fusion of information from two portable spectrometers for improved prediction of moisture and soluble solids content in pear fruit, *Talanta* 223 (2021) 121733, <https://doi.org/10.1016/j.talanta.2020.121733>.
- [24] P. Mishra, J.M. Roger, D.N. Rutledge, A. Biancolillo, F. Marini, A. Nordon, D. Jouan-Rimbaud-Bouveresse, MBA-GUI: A chemometric graphical user interface for multi-block data visualisation, regression, classification, variable selection and automated pre-processing, *Chemomet. Intel. Lab. Syst.* 205 (2020) 104139, <https://doi.org/10.1016/j.chemolab.2020.104139>.
- [25] P. Mishra, J.M. Roger, D.N. Rutledge, E. Woltering, SPORT pre-processing can improve near-infrared quality prediction models for fresh fruits and agro-materials, *Postharvest Biol. Technol.* 168 (2020) 111271, <https://doi.org/10.1016/j.postharvbio.2020.111271>.
- [26] L. Zhou, C. Zhang, Z. Qiu, Y. He, Information fusion of emerging non-destructive analytical techniques for food quality authentication: A survey, *TrAC Trends Anal. Chem.* 127 (2020) 115901, <https://doi.org/10.1016/j.trac.2020.115901>.
- [27] P. Mishra, J.-M. Roger, D. Jouan-Rimbaud-Bouveresse, A. Biancolillo, F. Marini, A. Nordon, D.N. Rutledge, Recent trends in multi-block data analysis in chemometrics for multi-source data integration, *TrAC Trends Anal. Chem.* 137 (2021) 116206, <https://doi.org/10.1016/j.trac.2021.116206>.
- [28] F. Mendoza, R. Lu, H. Cen, Comparison and fusion of four nondestructive sensors for predicting apple fruit firmness and soluble solids content, *Postharvest Biol. Technol.* 73 (2012) 89–98, <https://doi.org/10.1016/j.postharvbio.2012.05.012>.
- [29] Q. Liu, K.e. Sun, N. Zhao, J. Yang, Y. Zhang, C. Ma, L. Pan, K. Tu, Information fusion of hyperspectral imaging and electronic nose for evaluation of fungal contamination in strawberries during decay, *Postharvest Biol. Technol.* 153 (2019) 152–160, <https://doi.org/10.1016/j.postharvbio.2019.03.017>.
- [30] W. Saeys, N. Nguyen Do Trong, R. Van Beers, B.M. Nicolai, Multivariate calibration of spectroscopic sensors for postharvest quality evaluation: A review, *Postharvest Biol. Technol.* 158 (2019) 110981, <https://doi.org/10.1016/j.postharvbio.2019.110981>.
- [31] Y. Huang, R. Lu, K. Chen, Prediction of firmness parameters of tomatoes by portable visible and near-infrared spectroscopy, *J. Food Eng.* 222 (2018) 185–198, <https://doi.org/10.1016/j.jfoodeng.2017.11.030>.
- [32] M. Zude, B. Herold, J.-M. Roger, V. Bellon-Maurel, S. Landahl, Non-destructive tests on the prediction of apple fruit flesh firmness and soluble solids content on tree and in shelf life, *J. Food Eng.* 77 (2) (2006) 254–260, <https://doi.org/10.1016/j.jfoodeng.2005.06.027>.
- [33] R.J. Blakey, Management of avocado postharvest physiology, (PhD). University of Kwazulu-Natal Pietermaritzburg, 2011.
- [34] L.C. Erickson, Y. Kikuta, Ripening Hass avocado in high and low humidities, *California Avocado Soc.* 48 (1964) 90–91.
- [35] R.J. Barnes, M.S. Dhanoa, S.J. Lister, Standard Normal Variate Transformation and De-Trending of Near-Infrared Diffuse Reflectance Spectra, *Appl. Spectrosc.* 43 (5) (1989) 772–777, <https://doi.org/10.1366/0003702894202201>.
- [36] J.-M. Roger, J.-C. Boulet, M. Zeaiter, D.N. Rutledge, Pre-processing Methods☆. Reference Module in Chemistry, Molecular Sciences and Chemical Engineering, Elsevier, 2020.
- [37] R.W. Kennard, L.A. Stone, Computer Aided Design of Experiments, *Technometrics* 11 (1) (1969) 137–148, <https://doi.org/10.1080/00401706.1969.10490666>.
- [38] P. Geladi, B.R. Kowalski, Partial least-squares regression: a tutorial, *Anal. Chimica Acta* 185 (1986) 1–17, [https://doi.org/10.1016/0003-2670\(86\)80028-9](https://doi.org/10.1016/0003-2670(86)80028-9).
- [39] Wold, S. (1987). PLS Modeling with Latent Variables in Two Or More Dimensions.
- [40] B.-C. Deng, Y.-H. Yun, D.-S. Cao, Y.-L. Yin, W.-T. Wang, H.-M. Lu, Q.-Y. Luo, Y.-Z. Liang, A bootstrapping soft shrinkage approach for variable selection in chemical modeling, *Anal. Chimica Acta* 908 (2016) 63–74, <https://doi.org/10.1016/j.aca.2016.01.001>.
- [41] B.G. Osborne, Near-Infrared Spectroscopy in Food Analysis. In *Encyclopedia of Anal. Chem.* (2006).
- [42] O.B.O. Ashton, M. Wong, T.K. McGhie, R. Vather, Y. Wang, C. Requejo-Jackman, P. Ramankutty, A.B. Woolf, Pigments in Avocado Tissue and Oil, *J. Agri. Food Chem.* 54 (26) (2006) 10151–10158, <https://doi.org/10.1021/jf061809j>.
- [43] C. Paniagua, S. Posé, V.J. Morris, A.R. Kirby, M.A. Quesada, J.A. Mercado, Fruit softening and pectin disassembly: an overview of nanostructural pectin modifications assessed by atomic force microscopy, *Ann. Bot.* 114 (6) (2014) 1375–1383, <https://doi.org/10.1093/aob/mcu149>.
- [44] S. Posé, C. Paniagua, A.J. Matas, A.P. Gunning, V.J. Morris, M.A. Quesada, J. A. Mercado, A nanostructural view of the cell wall disassembly process during fruit ripening and postharvest storage by atomic force microscopy, *Trends Food Sci. Technol.* 87 (2019) 47–58, <https://doi.org/10.1016/j.tifs.2018.02.011>.
- [45] P. Chen, N.U. Jung, V. Giarola, D. Bartels, The Dynamic Responses of Cell Walls in Resurrection Plants During Dehydration and Rehydration, *Front. Plant Sci.* 10 (2020) 1698.
- [46] F. Ozdemir, A. Topuz, Changes in dry matter, oil content and fatty acids composition of avocado during harvesting time and post-harvesting ripening period, *Food Chem.* 86 (1) (2004) 79–83, <https://doi.org/10.1016/j.foodchem.2003.08.012>.
- [47] R. Pedreschi, V. Uarrotta, C. Fuentealba, J.E. Alvaro, P. Olmedo, B.G. Defilippi, R. Campos-Vargas, Primary Metabolism in Avocado Fruit, *Front. Plant Sci.* 10 (2019) 795, <https://doi.org/10.3389/fpls.2019.00795>.
- [48] R.J. Blakey, S.Z. Tesfay, I. Bertling, J.P. Bower, Changes in sugars, total protein, and oil in 'Hass' avocado (*Persea americana* Mill.) fruit during ripening, *J. Hortic. Sci. Biotechnol.* 87 (4) (2012) 381–387, <https://doi.org/10.1080/14620316.2012.11512880>.
- [49] B.G. Osborne, T. Fearn, P.H. Hindle, Practical NIR spectroscopy with applications in food and beverage analysis, Longman scientific and technical, 1993.
- [50] C. Villaseñor-Mora, P. Martínez-Torres, A. Gonzalez-Vega, S.E. Borjas-García, G. Espinosa, V.H. Hernandez, Correlation of Post-Harvest Avocado Ripening Process with the Thermal Emissivity Measured from the Peel, *Appl. Eng. Agric.* 33 (2) (2017) 267–272, <https://doi.org/10.13031/aea.11768>.
- [51] Landahl, S., Gonzalez, J., Van Linden, V., & De Baerdemaeker, J. (2005). THE ACOUSTIC IMPULSE-RESPONSE OF APPLES IN RELATION TO INTERNAL DAMAGE AND IN RELATION TO APOPLASTIC PH. Paper presented at the Acta Horticulturae.
- [52] Burdon, J., Lallu, N., Haynes, G., Francis, K., Patel, M., Laurie, T., & Hardy, J. (2015). RELATIONSHIP BETWEEN DRY MATTER AND RIPENING TIME IN 'HASS' AVOCADO. Paper presented at the Acta Horticulturae.